ISSN 1068-3356, Bulletin of the Lebedev Physics Institute, 2022, Vol. 49, Suppl. 1, pp. S89–S95. © Allerton Press, Inc., 2022.
Russian Text © The Author(s), 2022, published in Kvantovaya Elektronika, 2022, Vol. 52, No. 8, pp. 754–758.

DIFFRACTION OPTICS

Formation of 2D Image Contours in the Zeroth and Plus Second Diffraction Orders during Double Bragg's Diffraction

V. M. Kotov[a,*], S. V. Averin[a], A. A. Zenkina[a], and A. S. Belousova[a]

[a] *Fryazino Branch, Kotelnikov Institute of Radio Engineering and Electronics, Russian Academy of Sciences, Fryazino, Moscow oblast, 141190 Russia*

**e-mail: vmk277@ire216.msk.su*

Received April 7, 2022; revised June 22, 2022; accepted June 22, 2022

Abstract—The possibility of formation of a 2D optical image contour during double Bragg's diffraction simultaneously in two Bragg's orders is investigated. Transfer functions of Bragg's orders of double diffraction are obtained with account for ellipticity of optical beams and the curvature of wave surfaces of the crystal. The conditions for obtaining the image contour simultaneously in the zeroth and plus second Bragg's orders are determined. This is confirmed experimentally using the example of Fourier processing of the image transferred by radiation at a wavelength of 0.63 μm. Double Bragg's diffraction is realized based on an acousto-optic cell made of a uniaxial gyrotropic paratellurite crystal, which operates at an acoustic frequency of 20.3 MHz.

Keywords: double Bragg's diffraction, uniaxial gyrotropic crystal, transfer functions, separation of 2D image contour

DOI: 10.3103/S1068335622130036

1. INTRODUCTION

One of effective methods for improving the reliability of signal measurements is the measurement during the propagation of signals via two channels. This approach is used, for example, in detection of vibroacoustic and shock signals [1], recording of interferograms in a two-probe Fourier spectrometer [2], the search and detection of weak optical signals [3–5], and determination of correspondences in the images using descriptor structures [6]. Two-channel measurements make it possible, on the one hand, to correct effectively the errors in the channels, and on the other hand, to substantially reduce measuring errors, which ensures a higher reliability of measurements

In this study, we propose the application of this method for separating and recording the image contours; the formation of two channels is realized using a single acousto-optic (AO) filter. In our opinion, such systems are especially promising in detection of weak optical signals. The use of one instead of two filters makes it possible to reduce the mass, size, energy consumption, and cost of the system in the whole.

The possibility in principle of the formation of two channels using Bragg's diffraction is based on the existence of multiple Bragg's light scattering when as a result of diffraction, two or even three diffraction peaks appear apart of the zero peak [7–10]. Multiple regimes have already been used for a substantial frequency shift of an optical signal, in designing of optical logic elements [10], and so on. It should be noted that multiple diffraction has already been used for image processing including 1D [11] as well as 2D images [12]. However, only single-channel variants of processing have been considered. The idea of image processing using the zeroth and plus first diffraction orders was put forth in [13]. However, only two (tangential and collinear) variants of Bragg's diffraction were considered [13–16]. Both variants are axisymmetric. The features of these variants did not permit the realization of simultaneous processing of images. It turns out that multiple diffraction regimes have wider functional potentialities. Their transfer functions contain a large number of regions for processing 2D images, while the transfer functions of the tangential and collinear diffraction variants have only one suitable region. Precisely this feature of multiple diffraction regimes is used in this study.

This study is aimed at obtaining image contours in the zeroth and plus second diffraction orders in the course of double Bragg's diffraction. These orders are separated maximally in the angular space, which substantially reduces their mutual influence. It is assumed that diffraction occurs in a uniaxial gyrotropic

paratellurite (TeO_2) crystal; this AO material is widely used in practice owing to its unique optical and acoustic properties [17, 18]. Since multiple diffraction regimes are realized in paratellurite when light propagates almost along its optical axis, where the curvature of the wave surfaces of the crystal is manifested quite strongly, the curvature of surfaces is taken into account. In addition, we also take into account the ellipticity of crystal waves (i.e., the TeO_2 crystal is gyrotropic).

It will be shown below that the transfer functions of the two orders are different, which makes it possible to solve a wider range of problem (e.g., concentrate attention on some regions of the image using one channel and on other regions, using the other channel).

2. THEORY

We assume that image processing is performed using the Fourier method, i.e., the transformation of the image into the Fourier transform, the multiplication of the Fourier transform and the transfer function of the spatial filter, and the inverse Fourier transformation [19]. In practice, the direct and inverse Fourier transformations are performed using the input and output lenses, while the multiplication of the Fourier transform and the transfer function of the filter is performed by passing radiation in the form of the Fourier transform through the spatial filter. In our investigations, the role of the spatial frequency filter is played by an AO cell. For determining the filtering properties of the AO cell, we are using the spectral method that has been successfully used for calculating the filtering characteristics of the "conventional" Bragg diffraction with one order [13–16]. Following the spectral approach, we represent the optical field (including the field transferring the Fourier transform of the image) as a set of plane waves; in this case, all events of diffraction of plane waves from an acoustic wave occur independently from one another. All diffracted waves also form a set of plane waves [20]. Let us suppose that initial radiation formed as a Fourier transform is a set of plane waves $E_{inc}(\theta_m)$, where θ_m is the angle of orientation of the mth plane wave. The amplitudes of diffraction orders are described by expressions

$$E_0(\theta_m) = E_{inc}(\theta_m)H_0(\theta_m),$$

$$E_{+1}(\theta_m + K/k) = E_{inc}(\theta_m)H_{+1}(\theta_m),$$

$$E_{+2}(\theta_m + 2K/k) = E_{inc}(\theta_m)H_{+2}(\theta_m).$$

Here, E_0, E_{+1}, and E_{+2} are the amplitudes of the zeroth, plus first, and plus second diffraction orders; E_{inc} is the amplitude of the inccident radiation field; K and k are the wavenumbers of the acoustical and optical plane waves; H_0, H_{+1}, and H_{+2} are the transfer functions of the zeroth, plus first, and plus second diffraction orders. The existence of additional angular shifts in amplitudes E_{+1} and E_{+2} by K/k and $2K/k$ reflects the angular deviation of the direction of propagation of diffracted plane waves from the direction of propagation of incident waves as a result of Bragg's diffraction. If the amplitudes of plane waves forming incident radiation field E_{inc} are identical, the distributions of the diffracted waves coincide with the distributions of the corresponding transfer functions. In this case, transfer functions H_0, H_{+1}, and H_{+2} are connected with one another by the following system of differential equations [8, 11, 12]:

$$\begin{aligned} \frac{dH_0}{dz} &= -\frac{A_0}{2} H_{+1} \exp(i\eta_0 z), \\ \frac{dH_{+1}}{dz} &= \frac{A_0}{2} H_0 \exp(i\eta_0 z) - \frac{A_1}{2} H_{+2} \exp(i\eta_1 z), \\ \frac{dH_{+2}}{dz} &= -\frac{A_1}{2} H_{+1} \exp(-i\eta_1 z), \end{aligned} \tag{1}$$

where $A_0 = \delta f_{01}$; $A_1 = \delta f_{12}$;

$$\delta = \frac{\pi}{\lambda}\sqrt{\frac{M_2 P_{ac}}{LH}}$$

is the Raman–Nath parameter; λ is the light wavelength, M_2 is the AO quality of the material; L is the AO interaction length; H is the acoustic column height; P_{ac} is the acoustic power; z is the coordinate along which the AO interaction evolves; and η_0 and η_1 are the phase synchronism detunings of the plus first and

plus second orders, respectively. Coefficients f_{01} and f_{12} appearing in the expressions for A_0 and A_1 take into account the ellipticity of polarization of optical beams and are defined as

$$f_{01} = f_{10} = \frac{1 + \rho_0\rho_1}{\sqrt{1-\rho_0^2}\sqrt{1-\rho_1^2}},$$
$$f_{12} = f_{21} = \frac{1 + \rho_1\rho_2}{\sqrt{1-\rho_1^2}\sqrt{1-\rho_2^2}}, \quad (2)$$

where $\rho_{0,\,1,\,2}$ are the ellipticities of polarization of waves E_0, E_{+1}, and E_{+2}, respectively. It is especially important to take ellipticity into account when TeO_2 is used as the AO material because this crystal is gyrotropic. Solving system (1) in the standard manner (see, for example, [11–21]), we obtain

$$H_0 = \sum_k^3 a_k \exp(i\beta_k z),$$
$$H_{+1} = -\frac{2i}{A_0}\sum_k^3 a_k\beta_k \exp[i(\beta_k + \eta_0)z], \quad (3)$$
$$H_{+2} = -\frac{A_1}{A_0}\sum_k^3 \frac{a_k\beta_k}{\beta_k + \eta_0 + \eta_1}\exp[i(\beta_k + \eta_0 + \eta_1)z].$$

Here, $k = 1, 2, 3$; β_k are the roots of cubic equation

$$\beta^3 + \beta^2(2\eta_0 + \eta_1) + \beta[\eta_0(\eta_0 + \eta_1) - 0.25(A_0^2 + A_1^2)]$$
$$-0.25A_0^2(\eta_0 + \eta_1) = 0; \quad (4)$$

$$a_k = \Delta a_k / B;$$
$$\Delta a_1 = \beta_2\beta_3[(\beta_3 + \eta_0 + \eta_1)^{-1} - (\beta_2 + \eta_0 + \eta_1)^{-1}];$$
$$\Delta a_2 = \beta_1\beta_3[(\beta_1 + \eta_0 + \eta_1)^{-1} - (\beta_3 + \eta_0 + \eta_1)^{-1}]; \quad (5)$$
$$\Delta a_3 = \beta_1\beta_2[(\beta_2 + \eta_0 + \eta_1)^{-1} - (\beta_1 + \eta_0 + \eta_1)^{-1}];$$
$$B = \Delta a_1 + \Delta a_2 + \Delta a_3.$$

As in [12], we will take into account the two-dimensional nature of transfer functions using the 3D representation of refractive indices of a uniaxial gyrotropic crystal [22]:

$$\eta_{1,2}^2 = \frac{1 + \tan^2\varphi}{\frac{1}{n_o^2} + \frac{\tan^2\varphi}{2}\left(\frac{1}{n_o^2} + \frac{1}{n_e^2}\right) \pm \frac{1}{2}\sqrt{\tan^4\varphi\left(\frac{1}{n_o^2} + \frac{1}{n_e^2}\right)^2 + 4G_{33}^2}}, \quad (6)$$

where n_o, n_e are the principal refractive indices of the crystal; φ is the angle between the optical axis of the crystal and the wavevector of the light wave, and G_{33} is the gyration pseudotensor component. Essentially, the three-dimensional form of the refractive indices determines the 3D distribution of phase detunings η_0 and η_1 [12]. Polarization ellipticities $\rho_{0,\,1,\,2}$ of the beams were calculated using expression

$$\rho = (2G_{33})^{-1}(\sqrt{T^2 + 4G_{33}^2} - T), \quad (7)$$

where $T = \sin^2\varphi(n_o^{-2} - n_e^{-2})$. In concrete calculations, we assumed that light wavelength $\lambda = 0.63$ μm (experimental condition). As the AO material, we used a TeO_2 crystal; accordingly, the parameters appearing in expressions (1)–(7) were as follows [23, 24]: $n_o = 2.26$, $n_e = 2.41$, $G_{33} = 2.62 \times 10^{-5}$, $M_2 = 1200 \times 10^{-18}$ s^3/g, and $V = 0.617 \times 10^5$ cm/s. The AO interaction length was $L = 0.2$ cm, the acoustic power was $P_{ac} = 0.175$ W, and the frequency of sound was 21 MHz. We assumed that the acoustic wave propagated along crystallographic axis [110] of paratellurite, while the optical axis of the crystal was the [001] axis. Transfer functions H_0, H_{+1}, and H_{+2} were constructed depending on angles α and β, where angle α was calculated in the ([110], [001]) plane from optical axis [001], while angle β was calculated in the ([1 $\bar{1}$0], [001]) plane also from optical axis [001]. Here, the [1 $\bar{1}$0] direction is orthogonal to directions [110] and [001].

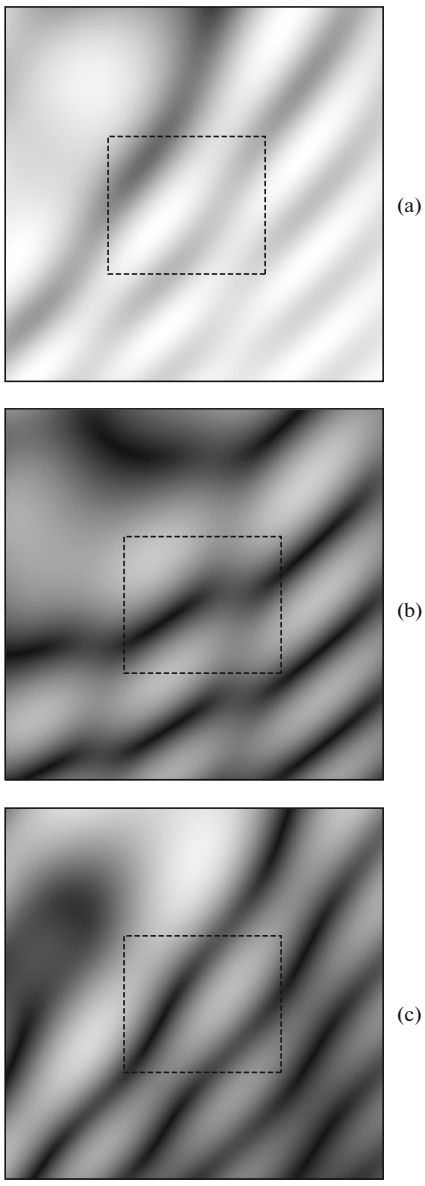

Fig. 1. Moduli of transfer functions of the zeroth (a), plus first (b), and plus second (c) Bragg's diffraction orders.

Calculations show that for small angles β, the field distributions during the variation of angle α are alternations of interference fringes. Such a distribution is characteristic of conventional Bragg's diffraction regimes with one order [8] and can be suitable only for 1D processing of images. With increasing angle β, the interference fringes become curved, bent, change their thickness, terminate, are transformed into loops, and so on. This is typical of only multiple diffraction regimes. As shown in [25], only regions with strong inhomogeneities are suitable for processing 2D images. Therefore, such regions should be sought at the periphery of transfer functions (i.e., for large angles β).

We sought the suitable regions of transfer functions, in which the reference center for angle β was shifted from 0 to about 7°. The determined regions are shown in Fig. 1. The angular size of the distributions is ~ 5° × 5°. Within each distribution, squares of size ~2° × 2° single out the working regions used for 2D Fourier processing of images. Calculations show that the distributions in Figs. 1a and 1c ensure the separation of a 2D contour, while the distribution in Fig. 1b does not in spite of its similarity to the distributions in Figs. 1a and 1c. It should be noted that the conclusion concerning the suitability of a certain region of the transfer function for the separation of a 2D contour can be drawn only after its verification based on the computer Fourier processing of images.

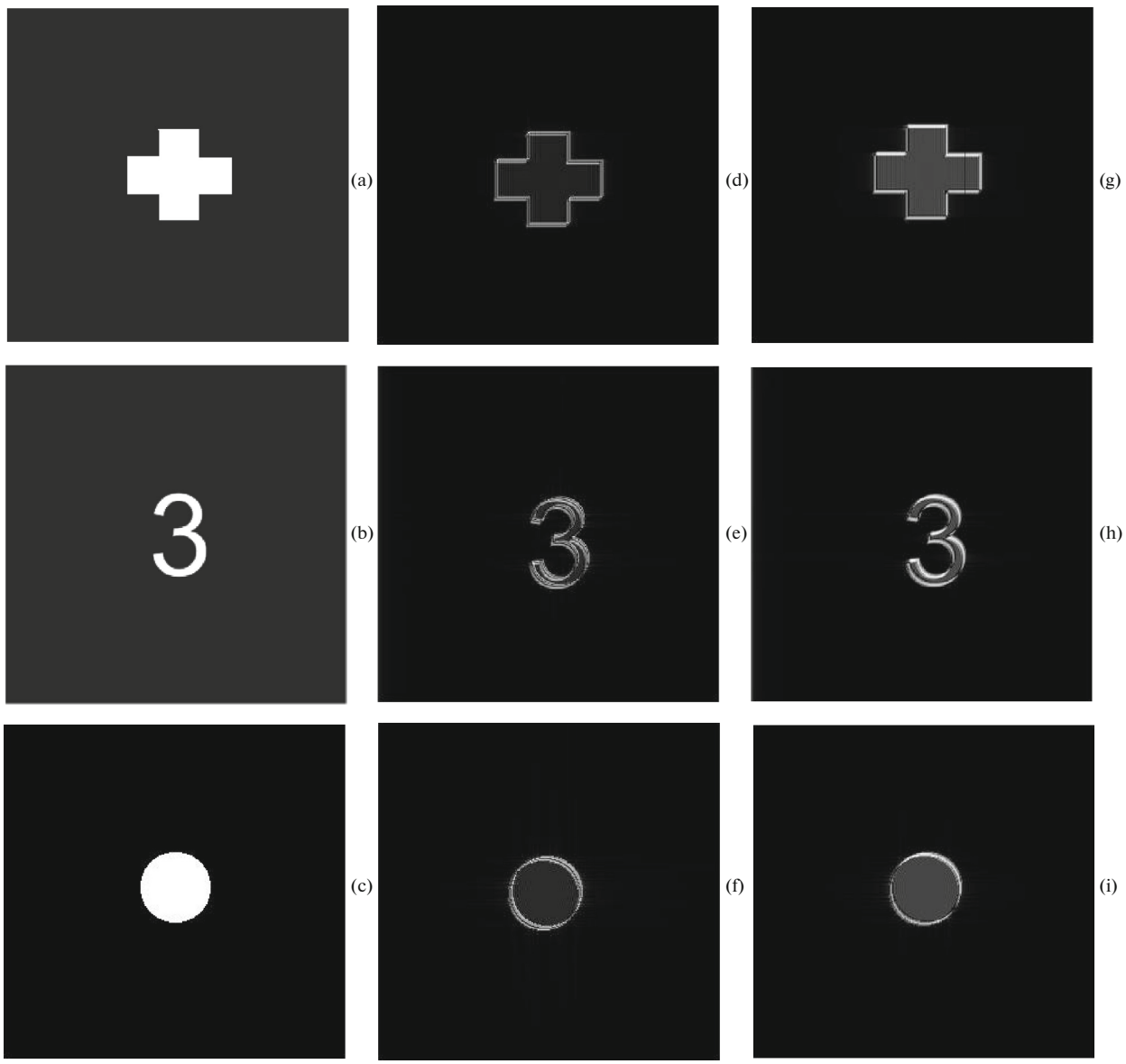

Fig. 2. Initial images (a, b, c) and the images obtained after processing using the transfer functions of the zeroth (d, e, f) and plus second (g, h, i) diffraction orders.

Figure 2 shows the results of Fourier processing of images using transfer functions H_0 and H_{+2}. The left column contains initial images in the form of a cross, figure 3, and a circle; the central and right columns contain the results of processing of these images with the help of transfer functions H_0 and H_{+2}, respectively. It can be seen that quite clear 2D contours of images are formed. The computer Fourier processing shows that the transfer functions with the distributions shown in Figs. 2a and 2c make it possible to separate a 2D contour, while the distribution shown in Fig. 2b does not. If, however, we shift all regions by 1°, the reverse situation takes place (the distribution in Fig. 2b ensures the separation of the contour, while the distributions in Figs. 2a and 2c do not).

Comparison of Figs. 2f and 2i shows that the zeroth-order contour (Fig. 2f) is sharper and has a higher contrast as compared to the contour of the plus second order (Fig. 2i); the latter is not so sharp; the regions in the central part of the image are suppressed more weakly than analogous regions of the zeroth diffraction order. Nevertheless, the image contour in both cases is separated clearly. In both contours, discontinuities can be distinguished; however, one can use other regions of transfer functions and obtain contours without discontinuities. We deliberately selected these regions of transfer functions to demonstrate wider

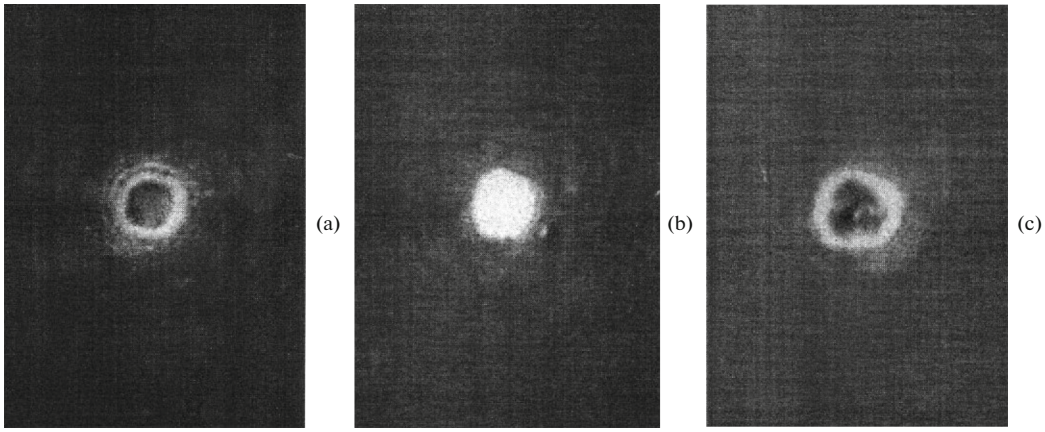

Fig. 3. Images observed on the screen in the zeroth (a), plus first (b), and plus second (c) diffraction orders.

potentialities of the two-channel method of separation of contours. In particular, this method makes it possible not only to form the same contour in two channels, but also to single out more clearly some regions of the contour using one channel and other regions, using the other channel.

3. EXPERIMENT

The separation of a 2D image contour in the zeroth and plus second Bragg's orders during double Bragg's diffraction was demonstrated experimentally. We used the standard 4*f* scheme of the Fourier processing (see, for example, [12]), which was based on two (input and output) identical lenses with focal length *f*. In our experiments, *f* was equal to 18 cm. The input image was a circular aperture in the screen made of an opaque material, which was separated from the input lens by distance *f*. The radiation source was a He–Ne laser generating radiation with a wavelength of 0.63 μm. The spatial frequency filter made of TeO_2 was located in the back focal plane of the input lens and simultaneously (in accordance with the setup design) in the front focal plane of the other (output) lens. The sizes of the AO filter along the [110], $[1\,\bar{1}0]$, and [001] directions were 1.0, 0.8, and 0.8 cm, respectively. A transverse acoustic wave propagated along the [110] direction of the crystal, while optical radiation propagated near the [001] optical axis. The acoustic frequency was chosen at 20.3 MHz. The formation of three diffraction orders was observed on the screen located in the back focal plane of the output lens. By smooth rotation of the AO filter around the [110] and $[1\,\bar{1}0]$ axes of the crystal and by variation of the voltage applied to the transducer, the conditions were created, in which a 2D image contour was formed in the zeroth and plus second Bragg's orders. The contours in the two orders were obtained at a voltage of 8.2 V.

Figure 3 shows the photographs of the images observed on the screen. It can be seen that quite clear 2D image contours have been formed in the zeroth and plus second diffraction orders. It can be seen above all that, generally speaking, the contours are different and not repeat each other. However, we assume that these contours successfully supplement each other (the features of one contour are not repeated in the other one). Therefore, the possibility of formation of a 2D contour simultaneously in the zeroth and plus second Bragg's orders as a result of double Bragg's diffraction has been confirmed experimentally. In our opinion, good agreement has been attained between the experimental results and the conclusions of the theory.

4. CONCLUSIONS

The results obtained in this study lead to the following conclusions.

1. The filtering properties of double Bragg's diffraction for the problem of separation of a 2D contour using two diffraction orders have been investigated. Based on the AO interaction model taking into account the ellipticity of natural waves and the curvature of the wave surfaces of a uniaxial gyrotropic crystal, transfer functions have been obtained for all diffraction orders.

2. The regime of the double AO interaction in a paratellurite crystal has been determined, in which the transfer functions of the zeroth and plus second diffraction orders ensure the formation of a 2D image contour.

3. The separation of a 2D image contour transferred by optical radiation with a wavelength of 0.63 μm in the zeroth and plus second diffraction orders has been performed experimentally using the optical Fourier processing. The role of the spatial frequency filter has been played by an AO paratellurite cell in which an acoustic wave is excited at a sound frequency of 20.3 MHz.

These results can be applied in processing of optical images, in which AO cells are used as spatial frequency filters.

FUNDING

This study was supported by the Russian Science Foundation (project no. 22-21-00059).

CONFLICT OF INTERESTS

The authors declare that they have no conflict of interests.

REFERENCES

1. Karelin, A.V., Len'kov, S.V., Molin, S.M., and Chekunov, D.V., *Pribory systemy. Upravlenie, kontrol, diagnostika*, 2008, no. 1, p. 46.
2. Vagin, V.A. and Khorokhorin, A.I., *Fizicheskie osnovy priborostroeniya*, 2019, vol. 8, no. 4(34), p. 11.
3. Bychkov, S.I. and Rumyantsev, K.E., *Poiks i obnaruzhenie opticheskikh signalov* (Search for and Detection of Optical Signals), Taganrog: TRTU, 2000.
4. Bogdanovich, V.A. and Vostretsov A.G., *Teoriya ustoichivogo obnaruzheniya, razlicheniya, i otsenivaniya signalov* (Theory of Stable Detection, Distinguishing, and Evaluation of Signals, Moscow: Fizmatlit, 2003.
5. Ampliev, A.E. and Rumyantsev K.E., *Izv. Vyssh. Uchebn. Zaved. Radioelektronika*, 2016, no. 5, p. 3.
6. Zakharov, A.A., Zhiznyakov, A.L., and Titov, V.S., *Kompyuternaya optika*, 2019, vol. 43, no. 5, p. 810.
7. Voloshinov, V.B., Parygin, V.N., and Chirkov, L.E., *Vestn. Mosk. Univ., Ser. 3: Fiz. Astron.*, 1976, vol. 17, no. 3, p. 305.
8. Balakshii, V.I., Parygin, V.N., and Chirkov, L.E., *Fizicheskie osnovy akustooptiki* (Physical Bases of Acoustooptics), Moscow: Radio i Svyaz, 1985.
9. Xu, J. and Stroud, R., *Acousto-Optic Devices: Principles, Design, and Applications,* New York: Wiley, 1992.
10. Rakovskii, V.Yu. and Shcherbakov, A.S., *Sov. Phys. Tech. Phys.*, 1990, vol. 60, no. 7, p. 107.
11. Kotov, V.M., Shkerdin, G.N., Shkerdin, D.G., Kotov, E.V., and Bulyuk A.N., *J. Commun. Technol. Electron.*, 2008, vol. 53, no. 3, p. 313.
12. Kotov, V.M., Shkerdin, G.N., and Grigor'evskii, V.I., *J. Commun. Technol. Electron.*, 2013, vol. 58, no. 3, p. 226.
13. Balakshii, V.I. and Voloshinov, V.B., *Quantum Electron.*, 2005, vol. 35, no. 1, p. 85.
14. Balakshy, V.I., Voloshinov, V.B., Babkina, T.M., and Kostyuk, D.E., *J. Mod. Opt.*, 2005, vol. 52, no. 1.
15. Balakshy, V.I. and Kostyuk, D.E., *Appl. Opt.*, 2009, vol. 48, p. C24.
16. Yablokova, A.A., Machikhin, A.S., Batshev, V.I., Pozhar, V.E., and Boritko, S.V., *Proc. SPIE*, 2019, vol. 11032, p. 1103215.
17. Uchida, N. and Ohmachi, Y., *J. Appl. Phys.*, 1969, vol. 40, no. 12, p. 4692.
18. Uchida, N., *Phys. Rev. B*, 1971, vol. 4, no. 10, p. 3736.
19. Goodman, J.W., *Introduction to Fourier Optics*, New York: McGraw-Hill, 1996.
20. Balakshii, V.I., Radiotekh. Elektron., 1984, vol. 29, no. 8, p. 1610.
21. Piskunov, N.S., *Differentsial'noe i integral'noe ischisleniya dlya vtuzov*. Vol. 2 (Differential and Integral Calculus for Technical Colleges. Vol. 2), Moscow: Nauka, 1970.
22. Kotov, B.M., *Akustooptika. Breggovskaya difraktsiya mnogotsvetnogo izlucheniya* (Acoustooptics. Bragg Diffraction of Multicolor Radiation), Moscow: Yanus-K, 2016.
23. *Akusticheskie kristally* (Acoustic Crystals), Shaskol'skii, M.P., Ed., Moscow: Nauka, 1982.
24. Kizel, V.A. and Burkov, V.I., *Girotropiya kristallov* (Crystal Gyrotropy), Moscow: Nauka, 1980.
25. Kotov, V.M., Averin, S.V., Kotov, E.V., and Shkerdin, G.N., *Appl. Opt.*, 2018, vol. 57, no. 10, p. C83.

Translated by N. Wadhwa